small
NANO MICRO

Spontaneous Formation of Heterogeneous Patches on Polymer–Lipid Core–Shell Particle Surfaces during Self-Assembly

*Carolina Salvador-Morales, Pedro M. Valencia, Weiwei Gao, Rohit Karnik, and Omid C. Farokhzad**

Nanoparticle (NP) surfaces have been widely investigated and engineered due to their importance in the synthesis of particles for targeted drug delivery, vaccination, medical imaging, as well as personal care products, and electronics.[1] For instance in drug delivery, the ability to functionalize the surface of NPs with ligands for differential delivery of drugs has demonstrated increased target cell uptake compared to equivalent NPs lacking the ligands.[2] Similarly, modification of the surface of inorganic NP such as quantum dots, iron oxide, and gold NPs, has been explored to render them biocompatible and non-toxic for applications in therapeutics and diagnostics.[3] Common methods used to characterize particle physicochemical properties include nuclear magnetic resonance (NMR), surface plasmon resonance (SPR), X-ray diffraction (XRD), and dynamic light scattering (DLS), among others.[4] However, while these techniques tend to measure the properties of a population of particles, they tend to overlook the surface characteristics of single particles such as ligand distribution and charge density distribution over the particle surface, which could greatly impact their expected interaction with cells, proteins or other particles.

Heterogeneous arrangement of ligands or functional groups on particle surfaces could result in the formation of clusters or 'patches', which may bestow the particle with different functionalities compared to those with uniformly distributed ligands. For instance, patchy particles can self-assemble into 2D and 3D structures of different sizes and shapes, which could be implemented for the self-assembly of devices in which instructions for assembly emerge from the nature of the forces acting between constituents, or it could bring insights to the thermodynamics and kinetics of molecule self-assembly at the atomic scale.[5] In the area of drug delivery patchy NPs presenting clusters of targeted ligands, have demonstrated to have higher efficacy than those NPs with homogenous distribution of the ligand around the surface, which may be attributed partly to the increased avidity due to clustering.[6] Finally, patchy NPs could be useful in the area of in vitro diagnostics where surface heterogeneity allows for simultaneous interaction with both a substrate and a reporter biomolecule, thus decreasing the number of components in the system.[7]

While the engineering of patchy particles has been widely investigated and several multi-step techniques have been developed (e.g. template-assisted fabrication,[8] evaporation-driven colloidal assembly,[9] particle lithography,[10] glancing-angle vapor deposition,[11] nanoparticle lithography,[12] and electrified jetting),[13] single step self-assembly of patchy particles has been less commonly observed. Indeed, surface heterogeneity of particles has been observed mostly for nanocrystals composed of metals such as selenium, cadmium, tellurium, zinc, and copper, among others.[14] For example, CdTe nanowires with heterogeneous surface properties were observed when organic coatings with two different structures and chemical properties were deposited onto the nanowire forming patches to minimize the surface energy.[15] However, for the case of organic particles such as polymeric or lipid-based NPs and microparticles (MPs) spontaneous formation of patches during or after self-assembly has not been observed.

Here, we report the visualization of patches formed on NP and MP surfaces of polymer-lipid hybrid particles exhibiting a core-shell structure. These particles contain a hydrophobic homogeneous core composed of poly(D,L-lactide-*co*-glycolide) (PLGA), and a hydrophilic shell composed of a mixture of lecithin and 1,2-distearoyl-sn-glycero-3-phosphoethanolamine (DSPE)-*N*-polyethylene glycol (PEG) with different terminal-functional groups, such as NH_2, OCH_3 and maleimide (MAL) that is physically adsorbed onto the PLGA core through hydrophobic-hydrophobic interactions.

Prof. C. Salvador-Morales,[+] Dr. W. Gao,
Prof. O. C. Farokhzad
Laboratory of Nanomedicine and Biomaterials
Department of Anesthesiology
Brigham and Women's Hospital-Harvard Medical School
Boston, MA 02115, USA
E-mail: ofarokhzad@zeus.bwh.harvard.edu
P. M. Valencia
Department of Chemical Engineering
Massachusetts Institute of Technology
Cambridge, MA 02139, USA
Prof. R. Karnik
Department of Mechanical Engineering
Massachusetts Institute of Technology
Cambridge, MA 02139, USA
[+] Current Address: Bioengineering Department, George Mason University, 4400 University Drive, MS 1G5, Fairfax, VA 22030, USA

DOI: 10.1002/smll.201201499

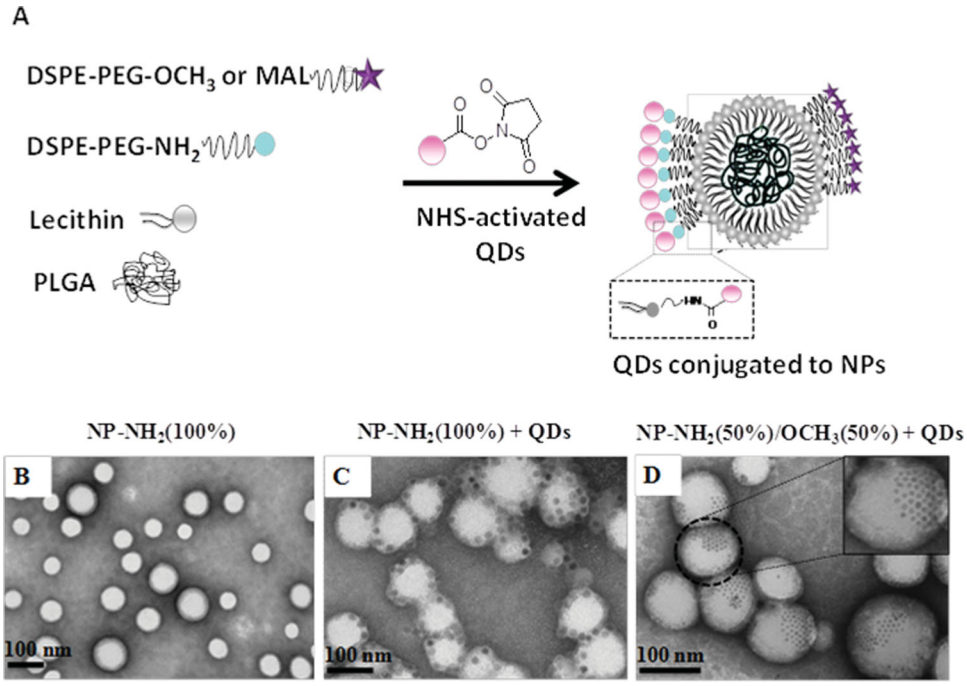

Figure 1. Formation of patchy NPs via a modified self-assembly process. A) Schematic diagram of the formation of NPs via self-assembly of DSPE-PEG terminated with NH_2 and OCH_3, lecithin, and the hydrophobic PLGA polymer. The distribution of the NH_2 functional groups was visualized with TEM through its conjugation with carboxylated quantum dots. B) NPs synthesized only with DSPE-PEG-NH_2. C) NPs-NH_2 traced with carboxylated quantum dots revealed the random distribution of the amino groups on NP surface. D) NPs synthesized with DSPE-PEG-NH_2 (50%) and DSPE-PEG-OCH_3 (50%) and traced with QDs revealed the patchy character of these particles.

In NPs, the formation of patches emerged from the segregation of DSPE-PEG-NH_2 and DSPE-PEG-OCH_3, and their visualization by TEM was accomplished by conjugating carboxylated quantum dots (QDs) to the NH_2 groups on the NP surface. Similarly patches were observed on MPs by conjugating gold NPs to NH_2 groups on the particle surface, or by the conjugation of a fluorescent dye to the MAL groups on DSPE-PEG-MAL prior to particle self-assembly. As proof-of-concept for taking advantage of this phenomenon for the synthesis of particles with multiple functionalities for potential biomedical applications, we conjugated two different bioactive proteins to NH_2 and MAL groups on a MP surface followed by visualization of protein clusters using confocal microscopy. Finally, we demonstrated synergistic binding of patchy particles with dual functionalization to B cells.

Our model particles are composed of a PLGA core and a shell composed of lecithin and DSPE-PEG with terminal functional groups NH_2, OCH_3, and MAL referred to as NPs-NH_2, NPs-OCH_3 and NPs-MAL, respectively. The formation of these particles involves a single mixing step where PLGA in an organic water-miscible solvent like acetonitrile is mixed with an aqueous solution containing lecithin and DSPE-PEG (**Figure 1**A).[16] Prior to preparing NPs with two functional groups, we first synthesized 80–100 nm NPs with a single surface functional group, NH_2, as previously reported by our group (Figure 1B).[17] Next, NHS-activated QDs of 5 nm in size were conjugated to the NH_2 groups on the particle surface to investigate their spatial distribution throughout the surface followed by their visualization through TEM. The resulting image shows evenly distributed QDs on the NPs-NH_2 particle surface, revealing the random localization of NH_2 on the NP surface (Figure 1C). Subsequently, we investigated the arrangement of two different functional groups on the particle surface by mixing DSPE-PEG-NH_2 and DSPE-PEG-OCH_3 at a 50% molar ratio in the aqueous solution followed by the same synthesis procedure as done for previous NPs. The presence of the NH_2 groups was identified by the immobilization of QDs, while the OCH_3 groups were unmodified. TEM images show clusters of quantum dots on the particle surface, which suggests the formation of patches formed by the clustering of DSPE-PEG-NH_2 chains (Figure 1D).

With the goal of investigating whether the formation of patches also occurred at the micron-scale instead of being a phenomenon displayed exclusively at the nano-scale, we prepared MPs with a similar composition through an emulsification-based method. In this method, PLGA was dissolved in ethyl acetate and the solution was then emulsified using a homogenizer with an aqueous solution that contained DSPE-PEG-NH_2 (50%), DSPE-PEG-MAL (50%) (molar ratio). After the organic solvent was evaporated, NH_2 groups were traced with 5-nm gold NPs followed by their visualization with TEM (**Figure 2**A) and SEM (Figure 2B). The dark region in Figure 2A demonstrates the presence of gold, which indicates the cluster formation of DSPE-PEG-NH_2 chains on the particle surface. SEM images also revealed the presence of NH_2 functional groups through the visualization of gold NPs. The patches on these MPs were much bigger than the ones observed for the NPs presumably due to the absence of

small 2012,
DOI: 10.1002/smll.201201499

NANO MICRO small

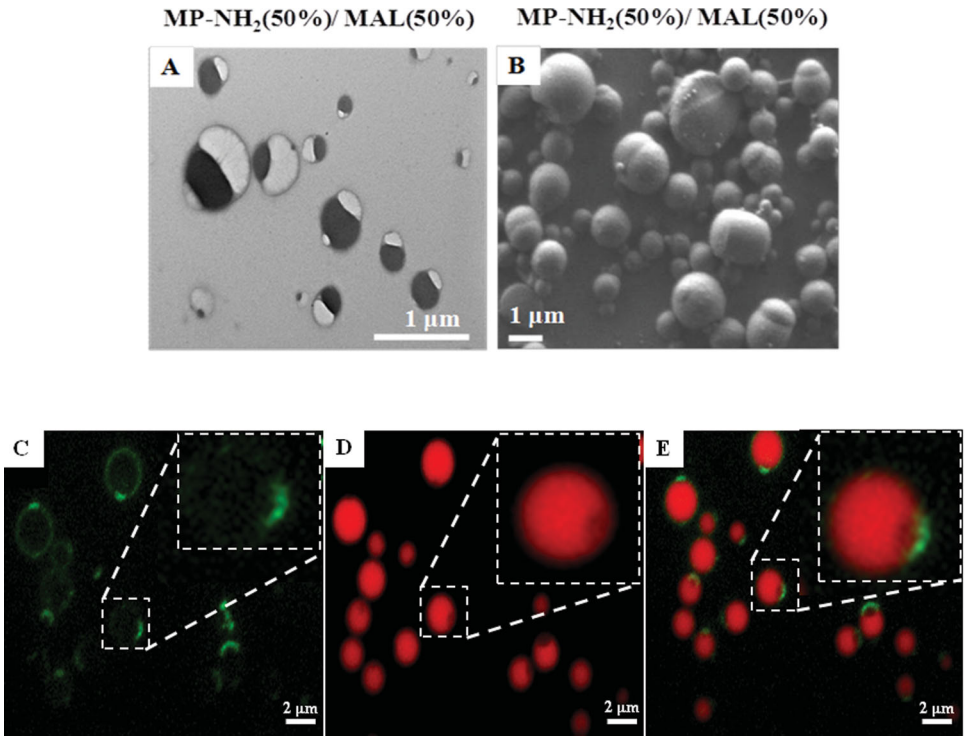

Figure 2. Characterization of patchy MPs with TEM, SEM and Confocal Laser Scanning Microscopy (CLSM). A) Unstained TEM image of patchy MPs synthesized with DSPE-PEG-NH_2 (50%) and DSPE-PEG-MAL (50%), where the gold NPs were conjugated to NH_2 groups on the MP surface (Dark region). B) SEM image of the above mentioned particles. C) CLSM image of patchy MPs synthesized via the emulsion method. MPs were synthesized with DSPE-PEG having two different functional groups (DSPE-PEG-NH_2 (50%)/DSPE-PEG-MAL(50%)). DSPE-PEG-MAL patch was labeled with SAMSA fluorescein (green), while DSPE-PEG-NH_2 patch was not labeled. D) Bodipy-X was encapsulated in the core for particle visualization (red). E) The overlay of the individual fluorescence channels shows the formation of patches on the MP surface.

lecithin and the increased amount of DSPE-PEG relative to PLGA.

To investigate whether the formation of patches is induced by the conjugation of gold NPs or QDs to NH_2 groups after particle formation rather than patch formation during particle self-assembly, we conjugated SAMSA fluorescein to the MAL group in DSPE-PEG-MAL chains before particle formation, followed by the formation of MPs composed of 50% DSPE-PEG-NH_2 and 50% DSPE-PEG-MAL through the previously described emulsification method (Figure 2C). In addition, we added the hydrophobic dye BODIPY-X to the PLGA organic solution to enable the visualization of the particle core by encapsulating the dye (Figure 2D). Confocal laser scanning microscopy was used to image both fluorescein on the particle surface and BODIPY-X in the particle core. Figure 2E shows the resulting MPs displaying patches located in one of the spheres' poles similarly to what was observed for MPs functionalized with gold NPs. These results suggest that segregation of surface functional groups into patches during self-assembly is a more general occurrence and not induced by conjugation of gold NPs or QDs after particle formation.

After discovering the formation of patches both on NPs and MPs, we evaluated if particles exhibiting patches with different functionalities could be synthesized by conjugating two biomolecules selectively onto different patches. Due to the limited resolution of the confocal microscope, bioconjugation was only carried out for MPs. In this study, a C3d fragment and a Hen Egg Lysozyme (HEL) were used as model biomolecules to attach on the surface of the particles. C3d is 35 kDa protein, member of the 35 complement proteins, and is an excellent natural adjuvant.[18] HEL is a 14 kDa model lysozyme, which is a protein that plays an important role in bacterial infections and other diseases.[19] Both biomolecules are of biological relevance in the synthesis of vaccines since C3d is a potent molecular adjuvant when conjugated to a soluble antigen[18] and HEL is a non-toxic antigen often used in animal models.[19,20] C3d was covalently attached to the NH_2 groups on the MPs surface using the Sulfo LC-SPDP spacer, while HEL was covalently attached to the MAL groups on the MPs via sulfide bond with thiol groups present in HEL (**Figure 3**A). A representative three-dimensional confocal microscopy image demonstrated the presence of C3d (blue) (Figure 3B) and HEL molecules (green) (Figure 3C) located on the MP surface. The presence of both proteins on different regions of the particle surface is an indication of the distribution of a number of MAL and NH_2 functional groups away from each other (Figure 3D). Interestingly, although in the particle formulation the ratio between MAL and NH_2 is 50/50, we observed greater coverage by C3d on the NP surface compared to the one observed by HEL. This is likely due to the interaction of the thiol groups present on C3d[21] with

DOI: 10.1002/smll.201201499

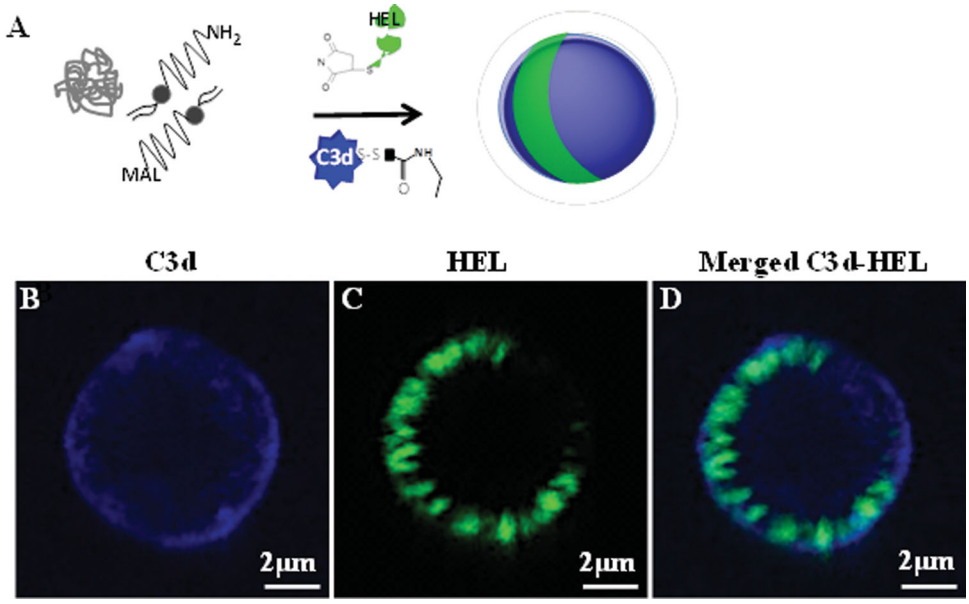

Figure 3. Schematic illustration of the formation of patchy MPs and their functionalization with C3d and HEL. A) 3D confocal microscopy of Patchy MPs. These particles were synthesized with DSPE-PEG-NH_2 (50%) and DSPE-PEG-MAL (50%), and were subsequently functionalized with C3d and HEL, respectively. CLSM images correspond to labeled C3d with Alexa 647 covalently attached to the NH_2 functional groups of MPs via the Sulfo-LC-spacer (B), labeled HEL with Alexa 488 covalently attached to the MAL groups via sulfide bond with thiol groups present in HEL (C). Overlay of C3d and HEL shows the presence of a patch formed by HEL biomolecules (D).

both the pyridinyldisulfide part of Sulfo-LC-SPDP crosslinker which was used to bind C3d covalently to NH_2 groups of the particles, and with MAL groups of the particles. HEL which has thiol groups on its surface interacts primarily with MAL groups of the MPs. Nevertheless, the fact that both proteins are present on the particle surface and that there are regions in which one type of protein formed clusters, could result in the generation of higher immune response compared to the one generated in the presence of only C3d or HEL.

Finally, as a proof of concept for the potential applications of these particles in the design of vaccines, we investigated the binding of patchy microparticles to B cells. These particles were functionalized with either Turkey Egg Lysozyme (an antigen and a homologous protein of HEL) and C3d (a natural adjuvant) or both proteins. Our hypothesis was that having both TEL and C3d on the same particle would potentially induce a higher immune response by B cells compared to administrating TEL and C3d in separate particles.

In vitro experiments were carried out with B Cells extracted from an MD4 transgenic mouse, which have overexpressed receptors specifically for TEL. In these experiments, we compared the uptake of particles having clusters of C3d, TEL or both on the surface. For detection, C3d and TEL were labeled with Alexa 647 and 488, respectively, and their interaction with B cells was measured by FACS. **Figure 4**a shows the fluorescent background of cells exposed to particles with no proteins on the surface. When B cells were incubated with particles containing C3d only (MP+C3d), an increase in C3d signal was observed for a low fraction of the cells (Figure 4b), presumably via the specific binding of C3d to CR2 receptor present in the surface of B cells. When cells were incubated with particles containing TEL only (MP+TEL), an increase in TEL signal was observed for most of the cells (Figure 4d) through the specific binding of TEL lysozymes to B cell receptors present in B cells. However, when MPs functionalized with clusters of both C3d and TEL (MP+C3d+TEL), a similar increase in signal was observed for TEL compared to MP+TEL, but now this time the signal for C3d was increased for a much larger fraction of the cells compared to MP+C3d (i.e. 6-fold increase; Figure 4c). The synergistic effect elicited by MP+C3d+TEL in B cells could potentially be useful to amplify the immune response since now higher titers of adjuvant C3d would be present in the cells. Further experiments will be needed to show the immune response induced by these particles, and therefore their use as a new type of vaccine.

These results demonstrate through different methods, the spontaneous formation of heterogeneous patches on NP and MP surfaces by coating them with relatively long lipid-polymeric chains differing only by their terminal group. This phenomenon was somewhat unexpected in light of the fact that NH_2 groups, having a positive charge at neutral pH, would tend to repel each other due to charge repulsion rather than forming clusters. A similar experimental observation was reported before[22,23] where it was found that charged and uncharged phospholipids segregated when blended and deposited on negatively charged silica beads.[22] In this case, it was concluded that the driving force for this phenomenon was mainly due to the electrostatic potential arising from the silica beads. The phase segregation phenomenon has also been observed in binary self-assembly monolayers (SAM) of n-alkanethiols on Au{111}[24,25] surfactant-coated

small 2012,
DOI: 10.1002/smll.201201499

NANO MICRO small

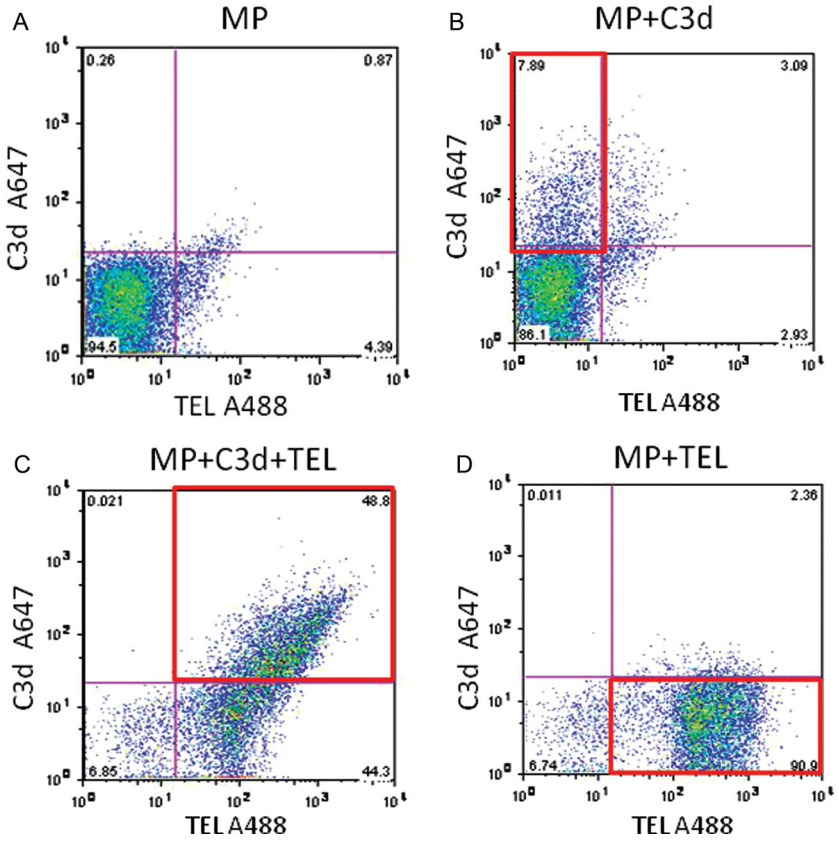

Figure 4. MD4 mouse B cells targeted by microparticles functionalized with labeled C3d, TEL and C3d+TEL. A) MP (fluorescent background of B cells exposed to particles with no fluorescent labeled proteins on the surface); B) MP+C3d (fluorescent signal of B cells exposed to particles containing only labeled C3d); C) MP+C3d+TEL (fluorescent signal of B cells exposed to particles containing both labeled C3d and TEL); D) MP+TEL (fluorescent signal of B cells exposed to particles containing only labeled TEL). The binding of MP+C3d to B cells is relatively low (8%), whereas the binding of MP+TEL to B cells is relatively high (91%), because of the specific binding of TEL lysozymes to B cell receptors in B cells. For particles with both C3d and TEL on their surface (MP+C3d+TEL), not only a similar percentage of B targeting by TEL occurs, but also the signal of C3d in B cells is increased by approximately 6-fold (49%).

nanoparticles and surfactant-coated flat substrates.[26] The mechanism involved in the formation of phase segregated domains in each of these cases is different. For example, in SAM phase segregation seems to be driven by factors such as the surface diffusion of the SAM onto the substrate (e.g. gold), thiol exchange, coalescence and motion of alkanethiolates.[24,25] In nanoparticles coated by two different surfactants, the curvature of the particles plays a key role in the formation of stripe-like domains and randomly distributed patches over the nanoparticle surface.[26] The higher the curvature of the substrate the most likely to observe wormlike stripes and randomly distributed patches over the surface.[26] In our study, the mechanism involved in the segregation of the lipid-pegylated functional groups is likely to be different, since the formation of patches seems to take place during the particle self-assembly rather than post-particle assembly. Also, other parameters such as the molecular weight of the DSPE-PEG-end functional group might have an influence in the formation of phase segregated domains. For example, high molecular weights (e.g. 10 000, 20 000 kDa) could cause the entanglement of PEG which might decrease its mobility, and thus impair segregation. In addition, other thermodynamics factors such as the minimization of energy might be involved in this phenomenon as previously observed in lipid segregation.[27] It is known that lipid layers tend to have lateral mobility in cell membranes and unilamelar vessels forming lipid 'rafts' that selectively interact with specific molecules.[28] Considering that DSPE forms a lipid monolayer on the PLGA core, it might be possible that lipids adsorbed rearrange themselves to form patches with the aim of minimizing surface energy. Further studies are needed to validate the abovementioned hypotheses and gain thorough understanding of the phase space where self-assembly occurs. While more effort should be devoted to understand and control the number and size of patches formed on a particle surface, this is a proof of concept of the creation of a new class of particles with multiple functionalities on a heterogeneous surface, and yet preserving a homogenous core for other purposes (e.g. encapsulation of agents). Equally important, these results present important implications for the future design of NPs or MPs that contain different groups on the surface. For instance, in drug delivery there are previous studies, including some from our own group, where polymers or lipids with different functional groups or ligands are mixed to obtain particles with different charge[17a] or ligand density.[29] While it has been previously assumed that ligands or charged groups are homogenously distributed throughout the particle surface, it might well be that ligand clusters or patches self-assembled on the particle surface potentially affect the behavior of the NPs. Specifically, in the case of particles that are coated with a fraction of lipids or polymers terminated with NH_2, positively charged patches could have been formed resulting in spots of high charge density that could increase the cytotoxicity of the particle and/or the interaction with blood proteins. In addition, in the case of targeted NPs formed by mixing ligand-conjugated polymers with unmodified ones,[29,30] clusters of ligands could be formed unexpectedly increasing or decreasing the uptake by the target cell.

Finally, further understanding of this phenomenon could result in the facile formation and engineering of patchy NPs with multiple functionalities that do not require multi-step and relatively elaborate methodologies. The fact that these particles are synthesized with clinically validated biomaterials such as PLGA, PEG and lipids, could enable the engineering and rapid clinical translation of multifunctional patchy NPs and MPs that can encapsulate a specific agent in their core and have multiple functionalities on their surface. A goal of future studies will focus on understanding what factors

DOI: 10.1002/smll.201201499

determine the size and number of patches on the particle surface and how they can be controlled for a specific application. In summary, we believe these findings are both important and exciting and should be taken into account as one of the particle design factors.

In conclusion, we report and demonstrate the spontaneous formation of patches on the surface of core-shell nanoparticles and microparticles. These patches were formed by the segregation of DSPE-PEG chains differing in functional end-groups that can be modified to have novel functionalities such as different biomolecules selectively presented on distinct patches on the surface. Patch formation was observed by TEM for NPs and TEM, SEM, and confocal microscopy for MPs. In vitro experiments show a synergistic effect created by the presence of two different proteins on the particle's surface. Finally, these findings could have important implications for the future design of self-assembled NPs and MPs for drug delivery carriers, and other biomedical applications.

Supporting Information

Supporting Information is available from the Wiley Online Library or from the author.

Acknowledgements

We thank Dr. Juliana Chan for helpful discussions and Thuy Tram Dang for assistance in developing the emulsification method. Also, we wish to thank Prof. Michael Carroll and Dr. Lisa A. Pitcher (Harvard Medical School) for providing Turkey Egg Lysozyme (TEL), excellent discussions on the vaccine application of patchy particles and technical assistance for the FACS experiments. This work was supported by the Koch- Prostate Cancer Foundation Award in Nanotherapeutics (O.C.F.), the NCI Center of Cancer Nanotechnology Excellence (U54- CA151884; O.C.F.), the NHLBI Programs of Excellence in Nanotechnology (HHSN268201000045C; O.C.F.), NIH 1R01EB015419-01 (O.C.F. and R.K), and CSM start-up fund (# 162904). P.M.V. is supported by NSF graduate research fellowship. O.C.F. discloses financial interest in BIND Biosciences, Selecta Biosciences and Blend Therapeutics, three biotechnology companies developing nanoparticle technologies for medical applications.

[1] a) D. Peer, J. M. Karp, S. Hong, O. C. Farokhzad, R. Margalit, R. Langer, *Nat. Nanotechnol.* **2007**, *2*, 751; b) J. A. Barreto, W. O'Malley, M. Kubeil, B. Graham, H. Stephan, L. Spiccia, *Adv. Mater.* **2011**, *23*, H18.

[2] N. Kamaly, Z. Xiao, P. M. Valencia, A. F. Radovic-Moreno, O. C. Farokhzad, *Chem. Soc. Rev.* **2012**, *41*, 2971.

[3] a) A. S. Karakoti, S. Das, S. Thevuthasan, S. Seal, *Angew. Chem. Int. Ed.* **2011**, *50*, 1980; b) R. Landsiedel, L. Ma-Hock, A. Kroll, D. Hahn, J. Schnekenburger, K. Wiench, W. Wohlleben, *Adv. Mater.* **2010**, *22*, 2601.

[4] a) D. R. Baer, D. J. Gaspar, P. Nachimuthu, S. D. Techane, D. G. Castner, *Anal. Bioanal. Chem.* **2010**, *396*, 983; b) T. Riley, C. R. Heald, S. Stolnik, M. C. Garnett, L. Illum, S. S. Davis, S. M. King, R. K. Heenan, S. C. Purkiss, R. J. Barlow, P. R. Gellert, C. Washington, *Langmuir* **2003**, *19*, 8428; c) E. Petryayeva, U. J. Krull, *Anal. Chim. Acta* **2011**, *706*, 8; d) J. Hrkach, D. Von Hoff, M. M. Ali, E. Andrianova, J. Auer, T. Campbell, D. De Witt, M. Figa, M. Figueiredo, A. Horhota, S. Low, K. McDonnell, E. Peeke, B. Retnarajan, A. Sabnis, E. Schnipper, J. J. Song, Y. H. Song, J. Summa, D. Tompsett, G. Troiano, T. Van Geen Hoven, J. Wright, P. Lorusso, P. W. Kantoff, N. H. Bander, C. Sweeney, O. C. Farokhzad, R. Langer, S. Zale, *Sci. Transl. Med.* **2012**, *4*, 128.

[5] a) Q. Chen, S. C. Bae, S. Granick, *Nature* **2011**, *469*, 381; b) Q. Chen, J. K. Whitmer, S. Jiang, S. C. Bae, E. Luijten, S. Granick, *Science* **2011**, *331*, 199.

[6] Z. Poon, D. Chang, X. Zhao, P. T. Hammond, *ACS Nano* **2011**, *5*, 4284.

[7] S. Bhaskar, C. T. Gibson, M. Yoshida, H. Nandivada, X. Deng, N. H. Voelcker, J. Lahann, *Small* **2011**, *7*, 812.

[8] a) A. Perro, F. Meunier, V. Schmitt, S. Ravaine, *Colloid Surface A* **2009**, *332*, 57; b) J. Q. Cui, I. Kretzschmar, *Langmuir* **2006**, *22*, 8281.

[9] a) V. N. Manoharan, M. T. Elsesser, D. J. Pine, *Science* **2003**, *301*, 483; b) Y. S. Cho, G. R. Yi, J. M. Lim, S. H. Kim, V. N. Manoharan, D. J. Pine, S. M. Yang, *J. Am. Chem. Soc.* **2005**, *127*, 15968.

[10] a) A. M. Yake, C. E. Snyder, D. Velegol, *Langmuir* **2007**, *23*, 9069; b) C. E. Snyder, A. M. Yake, J. D. Feick, D. Velegol, *Langmuir* **2005**, *21*, 4813.

[11] a) A. B. Pawar, I. Kretzschmar, *Langmuir* **2009**, *25*, 9057; b) A. B. Pawar, I. Kretzschmar, *Langmuir* **2008**, *24*, 355.

[12] a) G. Zhang, D. Wang, H. Mohwald, *Angew. Chem. Int. Ed.* **2005**, *44*, 7767; b) G. Zhang, D. Wang, H. Mohwald, *Nano Lett.* **2005**, *5*, 143.

[13] a) K. H. Roh, D. C. Martin, J. Lahann, *Nat. Mater.* **2005**, *4*, 759; b) K. H. Roh, D. C. Martin, J. Lahann, *J. Am. Chem. Soc.* **2006**, *128*, 6796.

[14] Z. Zhang, S. C. Glotzer, *Nano Lett.* **2004**, *4*, 1407.

[15] X. Liang, S. Tan, Z. Tang, N. A. Kotov, *Langmuir* **2004**, *20*, 1016.

[16] a) L. Zhang, J. M. Chan, F. X. Gu, J. W. Rhee, A. Z. Wang, A. F. Radovic-Moreno, F. Alexis, R. Langer, O. C. Farokhzad, *ACS Nano* **2008**, *2*, 1696; b) J. M. Chan, L. Zhang, K. P. Yuet, G. Liao, J. W. Rhee, R. Langer, O. C. Farokhzad, *Biomaterials* **2009**, *30*, 1627.

[17] a) C. Salvador-Morales, L. Zhang, R. Langer, O. C. Farokhzad, *Biomaterials* **2009**, *30*, 2231; b) P. M. Valencia, P. A. Basto, L. Zhang, M. Rhee, R. Langer, O. C. Farokhzad, R. Karnik, *ACS Nano* **2010**, *4*, 1671.

[18] P. W. Dempsey, M. E. Allison, S. Akkaraju, C. C. Goodnow, D. T. Fearon, *Science* **1996**, *271*, 348.

[19] M. C. Vaney, I. Broutin, P. Retailleau, A. Douangamath, S. Lafont, C. Hamiaux, T. Prange, A. Ducruix, M. Ries-Kautt, *Acta Crystallogr. D* **2001**, *57*, 929.

[20] C. C. Goodnow, J. Crosbie, S. Adelstein, T. B. Lavoie, S. J. Smith-Gill, R. A. Brink, H. Pritchard-Briscoe, J. S. Wotherspoon, R. H. Loblay, K. Raphael, R. J. Trent, A. Basten, *Nature* **1988**, *334*, 676.

[21] B. Nagar, R. G. Jones, R. J. Diefenbach, D. E. Isenman, J. M. Rini, *Science* **1998**, *280*, 1277.

[22] H. M. Reinl, T. M. Bayerl, *Biochem* **1994**, *33*, 14091.

[23] K. Kasbauer, M. Junglas, T. M. Bayerl, *Biophys. J.* **1999**, *76*, 2600.

[24] S. J. Stranick, A. N. Parikh, Y. T. Tao, D. L. Allara, P. S. Weiss, *J. Phys. Chem.* **1994**, *98*, 7636.

DOI: 10.1002/smll.201201499

[25] S. J. Stranick, S. V. Atre, A. N. Parikh, M. C. Wood, D. L. Allara, N. Winograd, P. S. Weiss, *Nanotechnology* **1996**, *7*, 438.
[26] C. Singh, P. K. Ghorai, M. A. Horsch, A. M. Jackson, R. G. Larson, F. Stellacci, S. C. Glotzer, *Phys. Rev. Lett.* **2007**, *99*, 226106.
[27] a) A. M. Jackson, J. W. Myerson, F. Stellacci, *Nat. Mater.* **2004**, *3*, 330; b) G. S. Longo, M. Schick, I. Szleifer, *Biophys. J.* **2009**, *96*, 3977.
[28] D. Lingwood, K. Simons, *Science* **2010**, *327*, 46.
[29] P. M. Valencia, M. H. Hanewich-Hollatz, W. W. Gao, F. Karim, R. Langer, R. Karnik, O. C. Farokhzad, *Biomaterials* **2011**, *32*, 6226.
[30] F. Gu, L. Zhang, B. A. Teply, N. Mann, A. Wang, A. F. Radovic-Moreno, R. Langer, O. C. Farokhzad, *Proc. Natl. Acad. Sci. USA* **2008**, *105*, 2586.

Received: June 30, 2012
Revised: August 29, 2012
Published online: